International Journal of Enhanced Research in Science, Technology & Engineering
ISSN: 2319-7463, Vol. 5 Issue 6, June-2016

Flow through a Layered Porous Configuration with Generalized Variable Permeability

M.S. Abu Zaytoon [1], T.L. Alderson [2], M.H. Hamdan [3]

[1,2,3] Dept. of Mathematics and Statistics, University of New Brunswick,
P.O. Box 5050, Saint John, New Brunswick, CANADA E2L 4L5
Corresponding Author: **hamdan@unb.ca**

ABSTRACT

Flow through a variable permeability porous layer, bounded by two constant-permeability layers is considered. Flow in governed by Brinkman's equation which is reduced to a generalized Airy's equation in the variable permeability layer for a particular choice of permeability function. Solutions are then obtained in terms of the generalized Airy's functions.

Keywords: Generalized Airy's Functions, Layered Porous Media, Transition Layer.

1. INTRODUCTION

In a series of articles, [1-4], coupled parallel flow through variable permeability porous layers has been considered. This type of flow is important in various industrial and natural applications that involve ground water recovery, flow of oil and gas, and in the design of cooling and heating systems, [5,6]. In particular, the problem of fluid flow through three layers with different permeability in each layer was previously considered, [1], where the middle layer was a variable-permeability transition layer. We assumed that the permeability in the middle layer to be a variable function of *y*, taken as a shifted rectangular hyperbola, while the bounding layers possessed constant permeability. The choice of variable permeability function was an idealization, by design, to result in an inhomogeneous Airy's ordinary differential equation whose solution is expressible in terms of the newly introduced Nield-Kuznetsov function [7,8,9]. The chosen permeability idealization is a subcase of the more general permeability function that is the reciprocal of a polynomial of degree *n*. The flow in the variable-permeability layer is then governed by a generalized inhomogeneous Airy's ordinary differential equation, [10].

In the current work, we consider flow through a transition layer bounded by two porous layer. This is the same configuration used in [1] except that the permeability in the transition layer is modelled in such a way that reduces the governing Brinkman's equation to a generalized Airy's differential equation. This approach offers a general approach to variable permeability modelling.

3. PROBLEM FORMULATION

Consider the steady flow of an incompressible viscous fluid in a composite of three porous layers, shown in **Fig. 1**. This is the same representative sketch used in [1], and the flow problem is governed by the same governing equations subject to the same boundary conditions. The only difference in the problem formulation is the description in the permeability distribution in the transition, middle layer, which we take in this work in a form that reduces Brinkman's equation to a generalized Airy's equation.

In order to illustrate the effects of this variable permeability function, we consider the same problem formulation as given in [1] and replace the permeability distribution with the more general permeability distribution, defined as follows:

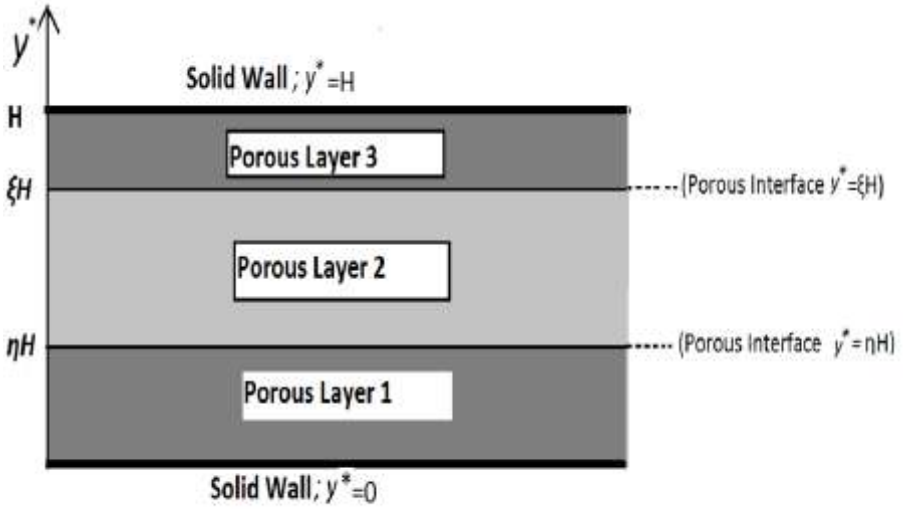

4.

Figure 1. Representative Sketch

For porous layer 1:

$$K_1 = aK_0; \text{for } 0 < y^* < \eta H. \tag{1}$$

For porous layer 2:

$$K_2(y^*) = abK_0\left[\frac{(\xi-\eta)H}{(\sqrt[n]{a}-\sqrt[n]{b})y^* + (\sqrt[n]{b}\xi - \sqrt[n]{a}\eta)H}\right]^n ; \text{for } \eta H < y^* < \xi H. \tag{2}$$

For porous layer 3:

$$K_3 = bK_0; \text{for } \xi H < y^* < H. \tag{3}$$

In equations (1), (2) and (3), K_0 is a reference constant permeability, *a* and *b* are constants to be selected as in *a=2* and *b=1*, ξ and η are parameters that determine the thickness of each layer. We note that at each interface between layers the permeability is continuous with $K_1 = K_2(\eta H) = aK_0$ and $K_3 = K_2(\xi H) = bK_0$. When *n=1,* we recover the permeability distribution of [1].

The governing equations and boundary conditions associated with the configuration in **Fig. 1** are stated as follows.

In layer 1, the flow is governed by:

$$\mu_{1eff}\frac{d^2u^*_1}{dy^{*2}} - \frac{\mu_1}{K_1}u^*_1 + G = 0 \ ; \ 0 < y^* < \eta H \tag{4}$$

In layer 2, the flow is governed by:

$$\mu_{2eff}\frac{d^2u^*_2}{dy^{*2}} - \frac{\mu_2}{K_2(y^*)}u^*_2 + G = 0 \ ; \ \eta H < y^* < \xi H \tag{5}$$

In layer 3, the flow is governed by:

$$\mu_{3eff}\frac{d^2u^*_3}{dy^{*2}} - \frac{\mu_3}{K_3}u^*_3 + G = 0 \ ; \ \xi H < y^* < H \tag{6}$$

In equations (4), (5) and (6), $G = -\frac{dp}{dx}$ is the common constant pressure gradient, $u_i^* = u_i^*(y^*)$ is the velocity in the ith layer, for *i=1,2,3,* K_i is the permeability in the ith layer, μ_i is the viscosity of the base-fluid saturating the ith

layer, and μ_{ieff} is the effective viscosity of the fluid in the ith layer. We note that the viscosities of the base fluids in the three layers should be equal, $\mu_1 = \mu_2 = \mu_3$, if the base fluid is the same. The effective viscosities, μ_{1eff}, μ_{2eff} and μ_{3eff} however, are not necessarily equal.

Now, introducing the dimensionless variables:

$$y = \frac{y^*}{H}; u_i = \frac{\mu_i}{GH^2} u^*_i \tag{7}$$

and defining $Da = \frac{K_0}{H^2}$ as the Darcy number, and $M_i = \frac{\mu_{ieff}}{\mu_i}$, equations (4), (5) and (6) take the following dimensionless forms, respectively:

$$M_1 \frac{d^2u_1}{dy^2} - \frac{H^2}{K_1} u_1 + 1 = 0 \; ; \quad 0 < y < \eta. \tag{8}$$

$$M_2 \frac{d^2u_2}{dy^2} - \frac{H^2}{K_2(y)} u_2 + 1 = 0 \; ; \quad \eta < y < \xi. \tag{9}$$

$$M_3 \frac{d^2u_3}{dy^2} - \frac{H^2}{K_3} u_3 + 1 = 0 \; ; \quad \xi < y < 1. \tag{10}$$

Now, substituting the permeability distribution, equations (1)-(3), in the dimensionless equations (8)-(10), respectively, we obtain the following form of governing equations:

$$\frac{d^2u_1}{dy^2} - \frac{1}{aDaM_1} u_1 + \frac{1}{M_1} = 0; 0 < y < \eta. \tag{11}$$

$$\frac{d^2u_2}{dy^2} - \frac{\left(\left(\sqrt[n]{a} - \sqrt[n]{b}\right)y + \left(\sqrt[n]{b}\xi - \sqrt[n]{a}\eta\right)\right)^n}{abDaM_2(\xi - \eta)^n} u_2 + \frac{1}{M_2} = 0; \eta < y < \xi. \tag{12}$$

$$\frac{d^2u_3}{dy^2} - \frac{1}{bDaM_3} u_3 + \frac{1}{M_3} = 0; \xi < y < 1. \tag{13}$$

In equation (12), *n* is a positive integer. The case when *n=1*, has been discussed in [1]. In this work we will assume that $n \geq 2$.

Equations (11), (12) and (13) are to be solved subject to the conditions of no-slip at the solid walls (*y = 0* and *y = 1*), velocity continuity and shear-stress continuity at the interfaces between layers ($y = \eta, \xi$), where the shear stress in each layer is defined based on the effective viscosity, namely $\mu_{ieff} \frac{du_i}{dy}$ for *i=1,2,3*. These conditions are stated as follows:

$$u_1 = 0 \text{ at } y = 0 \tag{14}$$

$$u_1 = u_2 \quad \text{at} \quad y = \eta \tag{15}$$

$$\frac{du_1}{dy} = \vartheta_1 \frac{du_2}{dy} \text{ at } y = \eta \tag{16}$$

$$u_2 = u_3 \quad \text{at} \quad y = \xi \tag{17}$$

$$\vartheta_2 \frac{du_2}{dy} = \frac{du_3}{dy} \quad \text{at} \quad y = \xi \tag{18}$$

$$u_3 = 0 \text{ at } y = 1 \tag{19}$$

where

$$\vartheta_1 = \frac{\mu_{2eff}}{\mu_{1eff}} \tag{20}$$

and

$$\vartheta_2 = \frac{\mu_{2eff}}{\mu_{3eff}}. \tag{21}$$

Solutions of equations (11) and (13) are given, respectively, by:

$$u_1(y) = a_1 \exp(\lambda_1 y) + a_2 \exp(-\lambda_1 y) + \frac{1}{M_1 \lambda^2_1} \tag{22}$$

$$u_3(y) = c_1 \exp(\lambda_3 y) + c_2 \exp(-\lambda_3 y) + \frac{1}{M_3 \lambda^2_3} \tag{23}$$

The values of λ_1, λ_2 are given below, and a_1, a_2, c_1, and c_2 are arbitrary constants that must be determined once equation (12) is solved and the boundary and matching conditions are implemented:

$$\lambda_1 = \frac{1}{\sqrt{aDaM_1}} \tag{24}$$

$$\lambda_3 = \frac{1}{\sqrt{bDaM_3}} \tag{25}$$

.

To solve equation (5), we first let

$$\omega_n = \frac{1}{\sqrt[n+2]{abM_2 Da(\xi-\eta)^n(\sqrt[n]{a}-\sqrt[n]{b})^2}} \tag{26}$$

and write equation (5) as

$$\frac{d^2u_2}{dy^2} - (\omega_a)^{n+2}(\sqrt[n]{a}-\sqrt[n]{b})^2[(\sqrt[n]{a}-\sqrt[n]{b})y + (\sqrt[n]{b}\xi - \sqrt[n]{a}\eta)]^n u_2 + \frac{1}{M_2} = 0. \tag{27}$$

Upon using the transformation $Y = \omega_n[\ (\sqrt[n]{a}-\sqrt[n]{b})y + (\sqrt[n]{b}\xi - \sqrt[n]{a}\eta)\ ]$, and writing $u_2(y) \equiv U_2(Y)$, we express (27) in the form:

$$\frac{d^2U}{dY^2} - Y^n U + \frac{1}{M_2(\sqrt[n]{a}-\sqrt[n]{b})^2 {\omega_n}^2} = 0 \tag{28}$$

where

$$\omega_n \sqrt[n]{b}(\xi - \eta) < Y < \omega_n \sqrt[n]{a}(\xi - \eta) \tag{29}$$

.

Equation (29) is a generalized inhomogeneous Airy's differential equation. Solution to the homogeneous part is a linear combination of the linearly independent functions $A_n(Y)$, and $B_n(\mathrm{Y})$, (cf. Swanson and Headley,[10]), namely

$$\mathrm{U}_{2h}(\mathrm{Y}) = b_1 A_n(\mathrm{Y}) + b_2 B_n(\mathrm{Y}) \tag{30}$$

where

$$A_n(\mathrm{Y}) = \frac{2p}{\pi} sin(p\pi)(\mathrm{Y})^{1/2} K_p(\zeta) \tag{31}$$

$$B_n(\mathrm{Y}) = (p\mathrm{Y})^{\frac{1}{2}}(I_{-p}(\zeta) + I_p(\zeta)). \tag{32}$$

The terms $I_p \; and \; K_p$ are the modified Bessel functions defined as:

$$I_p(\zeta) = i^{-p} J_p(i\zeta) = \sum_{m=1}^{\infty} \frac{1}{m!\,\Gamma(m+p+1)} (\frac{\zeta}{2})^{2m+p} \tag{33}$$

$$K_p(\zeta) = \frac{\pi}{2} \frac{\left(I_{-p}(\zeta) - I_p(\zeta)\right)}{\sin(p\pi)} \tag{34}$$

with $p = \frac{1}{n+2}$, $\zeta = 2pY$, and Γ is the gamma function.

The Wronskian of $A_n(\mathrm{Y})$ and $B_n(\mathrm{Y})$ is given by, [10]:

$$W\big(A_n(Y), B_n(\mathrm{Y})\big) = \frac{2}{\pi} p^{\frac{1}{2}} \sin(p\pi). \tag{35}$$

We note that $A_n(Y)$ and $B_n(Y)$ are Airy's functions $Ai(Y)$ and $Bi(Y)$, respectively, when $n = 1$.

3. SOLUTION METHODOLOGY

At this stage it is convenient to define the following integral function so as to parallel the Nield-Kuznetsov function, Ni(Y), [7]:

$$Z_n(\mathrm{Y}) = A_n(\mathrm{Y}) \int_0^Y B_n(t)dt - B_n(\mathrm{Y}) \int_0^{\mathrm{Y}} A_n(t)dt. \tag{36}$$

The function $Z_n(Y)$ reduces to Ni(Y) when $n = 1$. We will use this function to express the particular solution to (27), as follows. Using the method of variation of parameters, a particular solution of equation (27) is given by:

$$U_{2P}(\mathrm{Y}) = \frac{\pi}{2p^{\frac{1}{2}} \sin(p\pi)} Z_n(Y) \tag{37}$$

and the general solution takes the form:

$$U_2(\mathrm{Y}) = b_1 A_n(\mathrm{Y}) + b_2 B_n(\mathrm{Y}) + \frac{\pi}{2p^{1/2} sin(p\pi) M_2 (\sqrt[n]{a} - \sqrt[n]{b})^2 {\omega_n}^2} Z_n(\mathrm{Y}) \tag{38}$$

wherein b_1, b_2 are arbitrary constants.

The derivative of the functions $A_n(Y)$, $B_n(Y)$ and $Z_n(\mathrm{Y})$ are given, respectively, by (cf. [10]):

$$A_n'(Y) = -\frac{2p}{\pi} \sin(p\pi)\, Y^{\frac{n+1}{2}} K_{p-1}(\zeta) \tag{39}$$

$$B'(Y) = p^{\frac{1}{2}} (Y)^{\frac{n+1}{2}} \big[I_{1-p}(\zeta) + I_{p-1}(\zeta)\big] \tag{40}$$

and

$$Z_n'(Y) = A_n'(Y)\int_0^Y B_n(t)dt - B_n'(Y)\int_0^Y A_n(t)dt. \tag{41}$$

For convenience, and to simplify the appearance of equation (38), we let

$$\alpha_n = (\sqrt[n]{a} - \sqrt[n]{b}) \tag{42}$$

$$\beta_n = \left[\sqrt[n]{b}\xi - \sqrt[n]{a}\eta\right] \tag{43}$$

and

$$\varepsilon_n = \frac{\pi}{2p^{\frac{1}{2}}\sin(p\pi)M_2(\alpha_n\omega_n)^2}. \tag{44}$$

Equation (38) then becomes:

$$\begin{aligned} u_2(y) = b_1A_n\left(\omega_n(\alpha_n y + \beta_n)\right) + b_2B_n\left(\omega_n(\alpha_n y + \beta_n)\right) \\ + \epsilon_n Z_n\left(\omega_n(\alpha_n y + \beta_n)\right) \end{aligned} \tag{45}$$

with

$$\begin{aligned} \frac{du_2(y)}{dy} = b_1\omega_n\alpha_n A_n'\left(\omega_n(\alpha_n y + \beta_n)\right) + b_2\omega_n\alpha_n B_n'\left(\omega_n(\alpha_n y + \beta_n)\right) \\ + \epsilon_n\omega_n\alpha_n Z_n'\left(\omega_n(\alpha_n y + \beta_n)\right) \end{aligned} \tag{46}$$

We can further let:

$$\psi_n^1 = \omega_n\alpha_n \tag{47}$$

$$\psi_n^2 = \omega_n\beta_n \tag{48}$$

$$\psi_n^3 = \epsilon_n\omega_n\alpha_n \tag{49}$$

and express equations (45) and (46), respectively, as :

$$u_2(y) = b_1A_n\left(\psi_n^1 y + \psi_n^2\right) + b_2B_n\left(\psi_n^1 y + \psi_n^2\right) + \epsilon_n Z_n\left(\psi_n^1 y + \psi_n^2\right) \tag{50}$$

$$\frac{du_2}{dy} = b_1\psi_n^1 A_n'\left(\psi_n^1 y + \psi_n^2\right) + b_2\psi_n^1 B_n'\left(\psi_n^1 y + \psi_n^2\right) + \psi_n^3 Z_n'\left(\psi_n^1 y + \psi_n^2\right). \tag{51}$$

Equations (50) and (51) give us a compact form of the expressions of velocity and shear stress, respectively. Either equations (45) and (46) or equations (50) and (51) can be used in imposing boundary and interfacial conditions, and in the solution for the arbitrary constants. In what follows we will use equations (45) and (46).

3.1. Determining the Arbitrary Constants

Using the boundary and matching conditions, given by equations (14) to (19), we obtain:

$$a_1 + a_2 = -\frac{1}{M_1\lambda_1^2} \tag{52}$$

$$\begin{aligned} &a_1\exp(\lambda_1\eta) + a_2\exp(-\lambda_1\eta) - b_1A_n\left(\omega_n\sqrt[n]{b}(\xi-\eta)\right) - b_2B_n\left(\omega_n\sqrt[n]{b}(\xi-\eta)\right) \\ &= \epsilon_n Z_n\left(\omega_n\sqrt[n]{b}(\xi-\eta)\right) - \frac{1}{M_1}\lambda_1^2 \end{aligned} \tag{53}$$

$$b_1A_n\left(\omega_n\sqrt[n]{a}(\xi-\eta)\right) + b_2B_n(\omega_n\sqrt[n]{a}(\xi-\eta) - c_1\exp(\lambda_3\xi) - c_2\exp(-\lambda_3\xi) \tag{54}$$

$$= -\epsilon_n Z_n\left(\omega_n \sqrt[n]{a}(\xi-\eta)\right) + \frac{1}{M_3}\lambda_3^2$$

$$\begin{aligned}\lambda_1 a_1 \exp(\lambda_1\eta) - \lambda_1 a_2 \exp(-\lambda_1\eta) - b_1 \vartheta_1 \alpha_n \omega_n A_n'\left(\omega_n \sqrt[n]{b}(\xi-\eta)\right) \\ - b_2 \vartheta_1 \omega_n \alpha_n B_n'\left(\omega_n \sqrt[n]{b}(\xi-\eta)\right) \\ = \vartheta_1 \omega_n \alpha_n \epsilon_n Z_n'\left(\omega_n \sqrt[n]{b}(\xi-\eta)\right)\end{aligned} \quad (55)$$

$$\begin{aligned}&b_1\vartheta_2\omega_n\alpha_n A_n'(\omega_n \sqrt[n]{a}(\xi-\eta)) + b_2\vartheta_2\omega_n\alpha_n B_n'(\omega_n \sqrt[n]{a}(\xi-\eta)) + \vartheta_2\omega_n\alpha_n\varepsilon_n Z_n'(\omega_n \sqrt[n]{a}(\xi-\eta)) \\ &= c_1\lambda_3\exp(\lambda_3\xi) - c_2\lambda_3\exp(-\lambda_3\xi)\end{aligned} \quad (56)$$

$$c_1 \exp(\lambda_3) + c_2 \exp(-\lambda_3) = -\frac{1}{M_3\lambda_3^2} \quad (57)$$

where

$$\omega_n \sqrt[n]{b}(\xi-\eta) = \psi_n^1 \eta + \psi_n^2, \text{and } \omega_n \sqrt[n]{a}(\xi-\eta) = \psi_n^1 \xi + \psi_n^2.$$

Equations (52) through (57) represent a system of six equations in six unknowns that can be written in the matrix-vector form

$$MX = C \quad (58)$$

where

$$X = \begin{bmatrix} a_1 \\ a_2 \\ b_1 \\ b_2 \\ c_1 \\ c_2 \end{bmatrix}; \quad (59)$$

$$C = \begin{bmatrix} -\frac{1}{M_1\lambda_1^2} \\ \epsilon_n Z_n\left(\omega_n \sqrt[n]{b}(\xi-\eta)\right) - \frac{1}{M_1}\lambda_1^2 \\ \epsilon_n Z_n\left(\omega_n \sqrt[n]{a}(\xi-\eta)\right) - \frac{1}{M_3}\lambda_3^2 \\ \vartheta_1 \omega_n \alpha_n \epsilon_n Z_n'\left(\omega_n \sqrt[n]{b}(\xi-\eta)\right) \\ \vartheta_2 \omega_n \alpha_n \epsilon_n Z_n'\left(\omega_n \sqrt[n]{a}(\xi-\eta)\right) \\ -\frac{1}{M_3\lambda_3^2} \end{bmatrix} \quad (60)$$

and

$$M = \begin{bmatrix} 1 & 1 & 0 & 0 & 0 & 0 \\ \exp(\lambda_1\eta) & \exp(-\lambda_1\eta) & -A_n(\omega_n \sqrt[n]{b}(\xi-\eta)) & -B_n(\omega_n \sqrt[n]{b}(\xi-\eta)) & 0 & 0 \\ 0 & 0 & -A_n(\omega_n \sqrt[n]{a}(\xi-\eta)) & -B_n(\omega_n \sqrt[n]{a}(\xi-\eta)) & \exp(\lambda_3\xi) & \exp(\lambda_3\xi) \\ \lambda_1\exp(\lambda_1\eta) & -\lambda_1\exp(\lambda_1\eta) & -\vartheta_1\alpha_n\omega_n A'_n(\omega_n \sqrt[n]{b}(\xi-\eta)) & -\vartheta_1\alpha_n\omega_n B'_n(\omega_n \sqrt[n]{b}(\xi-\eta)) & 0 & 0 \\ 0 & 0 & -\vartheta_2\alpha_n\omega_n A'_n(\omega_n \sqrt[n]{a}(\xi-\eta)) & -\vartheta_2\alpha_n\omega_n B'_n(\gamma \sqrt[n]{a}(\xi-\eta)) & \lambda_3\exp(\lambda_3\xi) & -\lambda_3\exp(\lambda_3\xi) \\ 0 & 0 & 0 & 0 & \exp(\lambda_3) & \exp(-\lambda_3) \end{bmatrix} \quad (61)$$

An analytic solution to this system is rather involved and cumbersome. However, for given values of the functions and parameters, we can easily obtain numerical values for the constants, as will be explained in the following section of Results and Discussion.

4. RESULTS AND DISCUSSION

Solving governing equations (11)-(13) translates into calculating the velocity in each layer, subject to boundary and interfacial conditions. Transforming, non-dimensionalizing, and solving the resulting equations requires specifying and calculating flow parameters and problem-formulation parameters and arbitrary constants. These are specified and calculated below, in preparation for computing the velocity profiles and shear stress values across the layers.

4.1. Values of Parameters Involved

4.1.1. Choice of Permeability Parameters

We chosse $b < a$ so that $\omega_n \sqrt[n]{b}(\xi - \eta) < Y < \omega_n \sqrt[n]{a}(\xi - \eta)$ and, for the sake of illustration, we take in this work $a = 2$ and $b = 1$, so that parameter ω_n in equation (26) is well-defined for every value of the integer *n,* since all the quantities under the radical are positive.

4.1.2. Choice of the Integer *n*

An increase in the integer *n* influences (increases) the permeability value in the middle, variable-permeability layer. Although we will concentrate on results obtained for *n=2*, the method of analysis is valid for any value *n > 1.*

4.1.3. Choice of Layer Thickness

We choose the following layers thicknesses as representative of thick and thin layers, and layers of the same thickness:

(i) Layers are of equal thicknesses, where we choose $\eta = \frac{1}{3}$ and $\xi = \frac{2}{3}$.

(ii) Thick variable-permeability middle layer, where we choose without loss of generality $\eta = \frac{1}{4}$ and $\xi = \frac{3}{4}$.

(iii) Thin variable-permeability middle layer, where we choose without loss of generality $\eta = 0.49$ and $\xi = 0.51$.

4.1.4. Values of α_n and β_n

Parameters α_n and β_n have been defined by equations (42) and (43), respectively. Values of α_n, for $2 \le n \le 5$ are given in **Table 1**. Values of β_n for $2 \le n \le 5$ and the above range of layer thicknesses are shown in **Table 2**.

Table 1. Values of α_n for choices the integer *n*

n	α_n
n=2	0.414213562
n=3	0.259921050
n=4	0.189207115
n=5	0.148698355

Table 2. Values of β_n for choices of layer thicknesses and integer *n*

	n=2	n=3	n=4	n=5
$\eta = 1/3$ $\xi = 2/3$	β_2 =0.19526214	β_3 =0.2466929834	β_4 =0.2702642951	β_5 =0.2837672151
$\eta = 1/4$ $\xi = 3/4$	β_2 =0.3964466095	β_3 =0.4350197375	β_4 =0.4526982212	β_5 =0.4628254112
$\eta = 0.49$ $\xi = 0.51$	β_2 =-0.1829646454	β_3 =-0.107361314	β_4 =-0.072711486	β_5 =-0.0528621940

4.1.5. Choice of Effective Viscosities

We choose $\vartheta_1 = \vartheta_2 = 1$ and $M_i = \frac{\mu_{ieff}}{\mu_i} = 1, i = 1,2,3$, for illustration. However, the method of solution adopted in this work is still valid for different values of ϑ_1, ϑ_2 and M_i.

4.1.6. Choice of Darcy Number

We have chosen and tested the following range of values for the Darcy number *Da*: 1; 0.1; 0.01; 0.001; 0.0001; 0.00001. For low values of *Da*, computations become inaccurate. The most reliable results are found for *Da* greater than or equal to 0.001, hence are reported in this work.

4.1.7. Values of ω_n and ϵ_n

For *n = 2*, values of ω_n and ϵ_n, given by equations (26) and (44), have been calculated for various values of λ_1 ,and λ_3, and for choices of layer thicknesses and Darcy number. These values are given in **Table 3**.

Table 3. Values of λ_1, ω_2, ϵ_2 and λ_3 for choices of layer thicknesses and Darcy number

Da		Da=1	Da=0.1	Da=0.01	Da=0.001
$\eta = 1/3$ $\xi = 2/3$	λ_1	0.707107	2.2360689	7.071068	22.3606797
	λ_3	1	3.162278	10	31.622777
	ω_2	2.263033440	4.024305770	7.156340092	12.72597224
	ϵ_2	5.056317063	1.598947849	0.5056317063	0.1598947848
$\eta = 1/4$ $\xi = 3/4$	λ_1	0.7071067810	2.236067977	7.071067814	22.36067977
	λ_3	1	3.16227766	10	31.62277660
	ω_2	1.847759066	3.285831902	5.843127218	10.39071282
	ϵ_2	7.584475595	2.398421774	0.7584475591	0.2398421774
$\eta = 0.49$ $\xi = 0.51$	λ_1	0.707106781	2.236067977	7.07106781	22.360679
	λ_3	1	3.1622777	10	31.62277660
	ω_2	9.238795328	16.42915950	29.21563609	51.95356410
	ϵ_2	0.3033790241	0.09593687104	0.030337902	0.009593687

4.1.8. Values of ψ_n^1, ψ_n^2, and ψ_n^3

Parameters ψ_n^1, ψ_n^2, ψ_n^3, defined by equations (47), (48), and (49), respectively, have been calculated for choices of layer thicknesses and Darcy number, and presented in **Table 4.**

Table 4. Values of ψ_2^1, ψ_2^2, ψ_2^3 and for choices of layer thicknesses and Darcy number

	Da	Da=1	Da=0.1	Da=0.01	Da=0.001
$\eta = 1/3$ $\xi = 2/3$	ψ_2^1	0.9373791421	1.666922028	2.964253120	5.271270291
	ψ_2^2	0.4418847662	0.7857945812	1.397362325	2.484900651
	ψ_2^3	4.739686150	2.665321390	1.498820363	0.842848628
$\eta = 1/4$ $\xi = 3/4$	ψ_2^1	0.7653668644	1.361036136	2.420302538	4.303974169
	ψ_2^2	0.7325378169	1.302656917	2.316487974	4.119362868
	ψ_2^3	5.804906304	3.264338704	1.835672552	1.032274536
$\eta = 0.49$ $\xi = 0.51$	ψ_2^1	3.826834321	6.805180677	12.10151269	21.51987084
	ψ_2^2	-1.690372911	-3.005955342	-5.34542849	-9.50566543
	ψ_2^3	1.160981262	0.6528677410	0.367134510	0.206454907

4.2. Calculations of A_n, B_n and Z_n using the selected parameters

In order to calculate the arbitrary constants appearing in the velocity profile and shear stress terms, as shown in the next subsection, we need values of $A_2(\psi_n^1\eta + \psi_n^2)$, $B_2\left(\psi_n^1\eta + \psi_n^2\right)$, $Z_2\left(\psi_n^1\eta + \psi_n^2\right)$, $A_2'\left(\psi_n^1\eta + \psi_n^2\right)$, $B_2'\left(\psi_n^1\eta + \psi_n^2\right)$, *ψ n2, Z2′ψ n1η+ψ n2,A2ψ n1ξ+ψ n2,B2ψ n1ξ+ψ n2,Z2ψ n1ξ+ψ n2, A2′ψ n1ξ+ψ n2,B2′ψ n1ξ+ψ n2,Z2′ψ n1ξ+ψ n2.* These are the generalized Airy's functions *A2* and *B2* and their derivatives, and the integral function Z_2 and its derivative. They are calculated and tabulated in **Table 5(a-d)** for different Darcy number and layer thicknesses. **Table 5(a-d)** illustrate the extreme increases in these functions with decreasing Darcy number.

Table 5(a). Values of $A_2\left(\psi_n^1\eta + \psi_n^2\right), B_2\left(\psi_n^1\eta + \psi_n^2\right), Z_2\left(\psi_n^1\eta + \psi_n^2\right)$, for choices of layer thicknesses and Darcy number

	Da	Da=1	Da=0.1	Da=0.01	Da=0.001
$\eta = 1/3$ $\xi = 2/3$	A_2	0.146833896	0.065058886	0.0072952886	0.00001186707
	B_2	0.8917209197	1.353810836	6.560838905	2238.232882
	Z_2	-0.064732692	-0.22516722	-1.629536185	-572.2841478
$\eta = 1/4$ $\xi = 3/4$	A_2	0.1194469599	0.38374950	0.001603171	$-6.329393786\,10^{-7}$

	B_2	0.9861568103	1.87457561	24.16709524	$9.229602011\,10^5$
	Z_2	-0.098410257	-0.3837495	-6.149544169	$-2.359930057\,10^5$
$\eta = 0.49$ $\xi = 0.51$	A_2	0.2525057430	0.2246758878	0.1767009278	-0.1410989080
	B_2	0.6491680997	0.705837001	0.8118996417	0.7319688512
	Z_2	-0.00384248	-0.012155268	-0.038572894	-0.2617292710

Table 5(b). Values of $A_2'\left(\psi_n^1\eta + \psi_n^2\right), B_2'\left(\psi_n^1\eta + \psi_n^2\right), B_2'\left(\psi_n^1\eta + \psi_n^2\right), Z_2'\left(\psi_n^1\eta + \psi_n^2\right)_2$, for choices of layer thicknesses and Darcy number

Da		Da=1	Da=0.1	Da=0.01	Da=0.001
$\eta = 1/3$ $\xi = 2/3$	A_2'	-0.16918615	-0.106082395	-0.018777713	0.00005168606
	B_2'	0.505416316	1.252151498	13.96538664	9218.246192
	Z_2'	-0.17531794	-0.405704412	-3.616131622	-2357.032801
$\eta = 1/4$ $\xi = 3/4$	A_2'	-0.15337583	-0.072464982	-0.00493826	$-6.329393786\,10^{-7}$
	B_2'	0.618068962	2.332985064	65.95405078	$9.229602011\,10^5$
	Z_2'	-0.22330147	-0.67764337	-16.88836506	$-2.359930057\,10^5$
$\eta = 0.49$ $\xi = 0.51$	A_2'	-0.194481221	-0.192186413	-0.181465281	0.05242814112
	B_2'	0.3913894107	0.3980257861	0.439994757	1.536320030
	Z_2'	-0.041594038	-0.074043431	-0.133052950	-0.2827885351

Table 5(c). Values of $A_2\left(\psi_n^1\xi + \psi_n^2\right), B_2\left(\psi_n^1\xi + \psi_n^2\right), Z_2\left(\psi_n^1\xi + \psi_n^2\right)$, for choices of layer thicknesses and Darcy number

Da		Da=1	Da=0.1	Da=0.01	Da=0.001
$\eta = 1/3$ $\xi = 2/3$	A_2	0.09860649264	0.022958640	0.00036135186	$1.2408.10^{-9}$
	B_2	1.08432681	2.671724523	92.60297902	1.5122.107
	Z_2	-0.1336877333	-0.60691222	-23.65660180	$-3.8666.10^6$

$\eta = 1/4$ $\xi = 3/4$	A_2	0.06882950752	0.0085424722	0.000019070	$1.389871909\,10^{-13}$
	B_2	1.311585931	5.762401534	1430.166960	$1.102188867\,10^{11}$
	Z_2	-0.211393401	-1.422479637	-365.6678926	$-2.818202341\,10^{10}$
$\eta = 0.49$ $\xi = 0.51$	A_2	0.2376530136	0.1987990539	0.1348769032	0.05242814112
	B_2	0.6792099139	0.7609573701	0.9295310212	1.536320030
	Z_2	-0.007685874	-0.024338882	-0.078047397	-0.2827885351

Table 5(d). Values of for $A_2'\left(\psi_n^1\xi + \psi_n^2\right), B_2'\left(\psi_n^1\xi + \psi_n^2\right), Z_2'\left(\psi_n^1\xi + \psi_n^2\right)$ for choices of layer thicknesses and Darcy number

Da		Da=1	Da=0.1	Da=0.01	Da=0.001
$\eta = 1/3$ $\xi = 2/3$	A_2'	0.1380081301	-0.048745809	-0.0012695536	$-7.5455.10^{-9}$
	B_2'	0.7649918422	4.131067844	297.5344403	$8.943.10^{7}$
	Z_2'	-0.271968597	-1.126644226	-76.09151575	$-2.866.10^{7}$
$\eta = 1/4$ $\xi = 3/4$	A_2'	-0.110173205	0.021493363	-0.00008101	$-1.030518166\,10^{-12}$
	B_2'	1.170681799	11.84969502	5727.255599	$8.022071186\,10^{11}$
	Z_2'	-0.38451116	-3.07820516	-1464.417065	$-2.051174755\,10^{11}$
$\eta = 0.49$ $\xi = 0.51$	A_2'	-0.193542157	-0.18764106	-0.162856903	-0.09130406
	B_2'	0.3939496738	0.4139467720	0.5464133085	1.617581823
	Z_2'	-0.058843424	-0.105079381	-0.194740018	-0.49876870

4.3. Calculations of Values of Arbitrary Constants of Equation (6.40)

In order to determine velocity profiles and shear stress values, we must determine the arbitrary constants by solving equation (40). This requires using data in tables (**Table 1** to **Table 5)** in equation (40) to obtain a system that can be solved numerically to calculate the values of the constants $a_1, a_2, b_1, b_2, c_1, c_2$ .The values of the constants are tabulated in **Table 6** for different layer thickness and Darcy numbers. **Table 6** shows that some of the arbitrary constants attain extremely large values as Darcy number falls below 0.001, which implies unboundedness of the solution for the indicated small values of Da.

Table 6. Values of arbitrary constants, $a_1, a_2, b_1, b_2, c_1, c_2$, for choices of layer thicknesses and Darcy number

Da		Da=1	Da=0.1	Da=0.01	Da=0.001
$\eta = 1/3$ $\xi = 2/3$	a_1	-0.66445477	-0.0237808	-0.000218047	$5.7.10^{-8}$
	a_2	-1.33554522	-0.17621915	-0.019781952	-0.001999943
	b_1	-3.18353222	-1.8007126	-1.1623545	-11.975
	b_2	1.007705907	0.40141850	0.12928970	0.040883726
	c_1	-0.27000450	-0.00415849	$-4.5565.10^{-7}$	$-1.8477.10^{-17}$
	c_2	-0.72320342	-0.0415384	0.80453040	-0.27054064
$\eta = 1/4$ $\xi = 3/4$	a_1	-0.66458477	-0.024066376	-0.0002875593	0.000082
	a_2	-1.3354150	-0.17593362	-0.019712441	-0.002082
	b_1	-6.4488795	-4.2025049	-4.7571927	-3260
	b_2	1.6270872	0.60731433	0.19392830	0.061325704
	c_1	-0.27007734	-0.004168687	$-4.5654155\,10^{-7}$	$-1.8467278.10^{-17}$
	c_2	-0.72266492	-0.035850304	1.2168351	$-3.\,10^{12}$
$\eta = 0.49$ $\xi = 0.51$	a_1	-0.66443581	-0.023627378	-0.0001697113	$-8.1828222\,10^{-9}$
	a_2	-1.3355642	-0.17637261	-0.019830290	-0.0019999919
	b_1	0.16465943	0.11627925	0.025133581	-0.00064329179
	b_2	0.11637518	0.064325002	0.013158060	0.00064329179
	c_1	-0.26991787	-0.004147873	$-4.5512428\,10^{-7}$	$-1.8467279\,10^{-17}$
	c_2	-0.7238436	-0.047466486	0.54580252	3127.5428

4.4. Dimensionless Permeability Distribution

Permeability distributions for various values of *n*, Da, and thickness of the middle layer are illustrated in **Figures 2** and **3. Fig. 2(a,b)** illustrate the effects of increasing *n* on the permeability distribution in the variable permeability layer. Both graphs show the relative increase in permeability as *n* increases, for a given middle layer thickness and a given Darcy number. Effects of increasing Darcy number on the permeability distribution, for a given middle layer thickness and a given value of *n*, are illustrated in **Fig. 3(a,b)**. These

figures show the expected increase in permeability with increasing Darcy number.

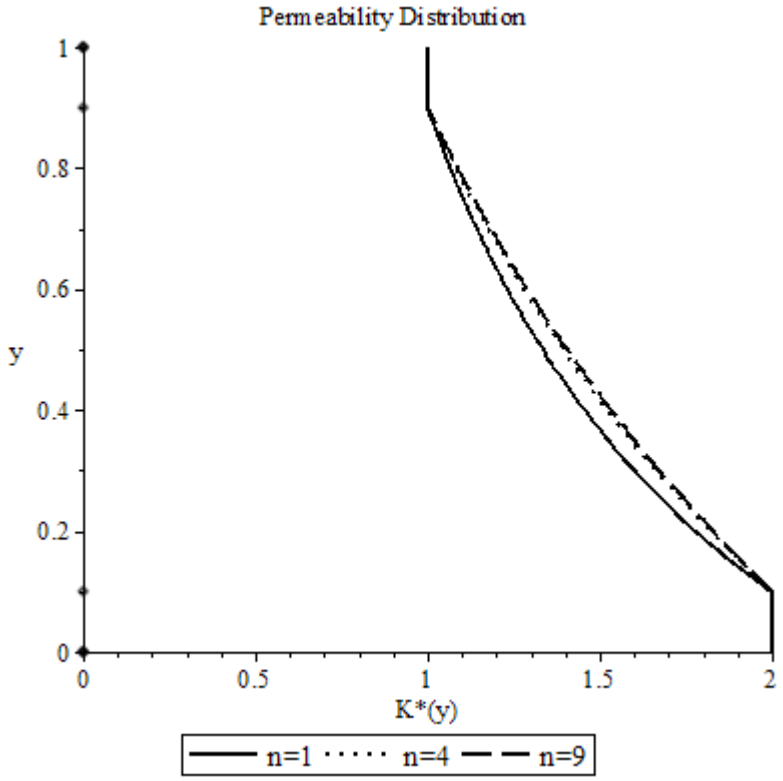

Figure 2(a): Permeability distribution *Da=1,* $\eta = 0.1, \xi = 0.9$ *, a=2,b=1* **and different values of** *n*.

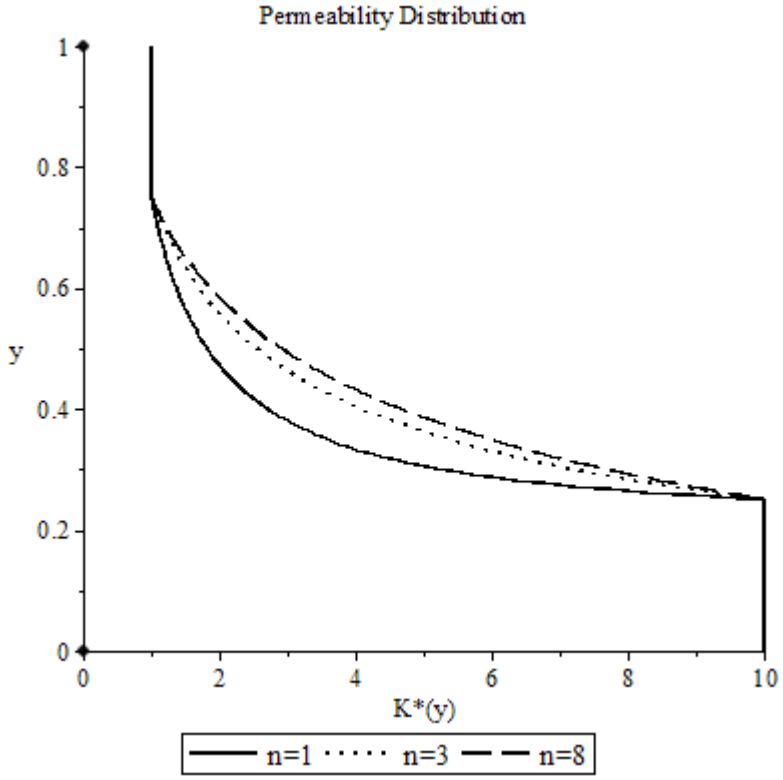

Figure 2(b): Permeability distribution *Da=1,* $\eta = 0.25, \xi = 0.75$ *, a=10,b=1,* **and different values of** *n*.

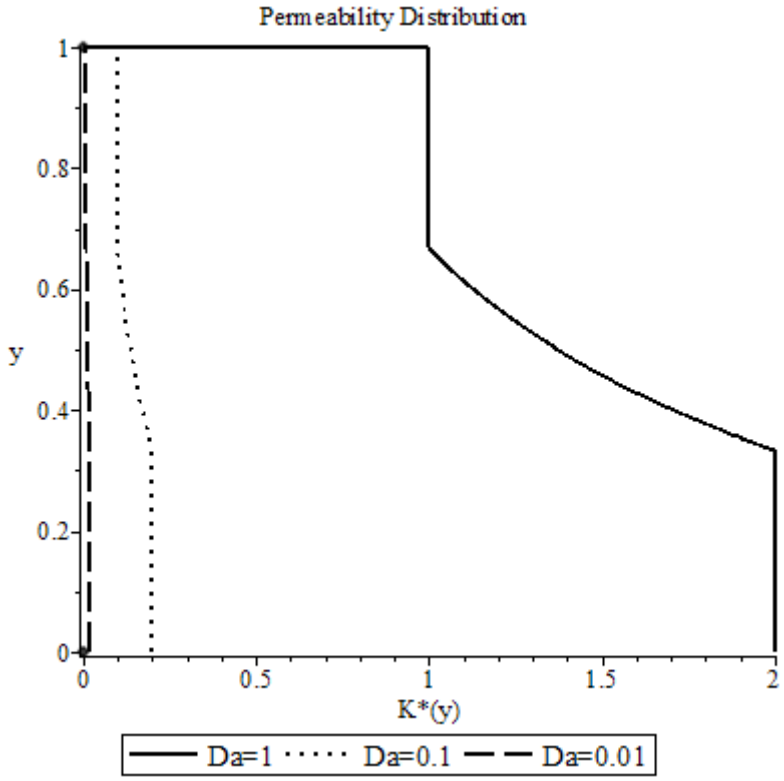

Figure 3(a): Permeability distribution *n=2,* $\eta = \frac{1}{3}, \xi = \frac{2}{3}$ *, a=2,b=1* **and different values of Darcy number.**

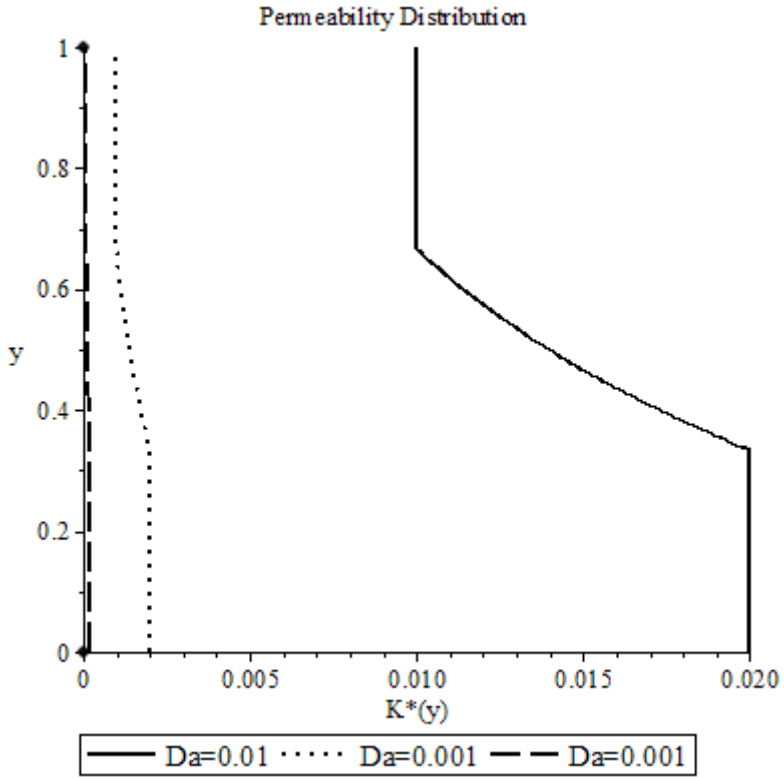

Figure 3(b): Permeability distribution *n=5,* $\eta = \frac{1}{3}, \xi = \frac{2}{3}$ *, a=2,b=1* **and different values of Darcy number.**

4.5. Velocity and shear stress computations at the interfaces between layers

Velocity and shear stress at the interfaces between the layers take the following forms:

$$u_2(\eta) = b_1 A_n\left(\psi^1_n \eta + \psi^2_n\right) + b_2 B_n\left(\psi^1_n \eta + \psi^2_n\right) + \epsilon_n Z_n\left(\psi^1_n \eta + \psi^2_n\right) \tag{62}$$

$$u_2(\xi) = b_1 A_n\left(\psi^1_n \xi + \psi^2_n\right) + b_2 B_n\left(\psi^1_n \xi + \psi^2_n\right) + \epsilon_n Z_n\left(\psi^1_n \xi + \psi^2_n\right) \tag{63}$$

$$\frac{du_2(\eta)}{dy} = b_1 \psi^1_n A_n'\left(\psi^1_n \eta + \psi^2_n\right) + b_2 \psi^1_n B_n'\left(\psi^1_n \eta + \psi^2_n\right) + \psi^3_n Z_n'\left(\psi^1_n \eta + \psi^2_n\right) \tag{64}$$

$$\frac{du_2(\xi)}{dy} = b_1 \psi^1_n A_n'\left(\psi^1_n \xi + \psi^2_n\right) + b_2 \psi^1_n B_n'\left(\psi^1_n \xi + \psi^2_n\right) + \psi^3_n Z_n'\left(\psi^1_n \xi + \psi^2_n\right) \tag{65}$$

Table 7(a) illustrates the velocity values at the lower and upper interfaces. This Table shows that for all choices of ξ and η the velocity values at the interfaces are very close to each other numerically whether the velocity expression used is that of the middle layer or that of an outer layer. This is true for high values of Darcy number. As *Da* reaches 0.001, inaccuracies start taking place and are caused by inaccuracies of computations and approximations of the Airy's functions, which in turn influence the computations of the arbitrary constants involved.

Similar conclusions are reached from **Table 7(b)**, which illustrates the shear stress values at the lower and upper interfaces and shows that inaccuracies start at *Da* = 0.001.

Table 7(a). Velocity at the lower and upper interfaces

Da		Da=1	Da=0.1	Da=0.01	Da=0.001
$\eta = 1/3$ $\xi = 2/3$	$u_1(\eta)$	0.1038331	0.06626168	0.015824149	0.0019004595
	$u_2(\eta)$	0.10383300	0.06626168	0.01582413	0.001903
	$u_2(\xi)$	0.10279805	0.06071672	0.010665	0.01
	$u_3(\xi)$	0.10279806	0.060716722	0.010665830	0.00099997336
$\eta = 1/4$ $\xi = 3/4$	$u_1(\eta)$	0.0878745	0.05731534	0.014950363	0.023950278
	$u_2(\eta)$	0.08787390	0.05731529	0.0149505	0.024
	$u_2(\xi)$	0.0868835	0.0519834	0.00985	13400.
	$u_3(\xi)$	0.08688353	0.051984085	0.009847566	150.28669
$\eta = 0.49$ $\xi = 0.51$	$u_1(\eta)$	0.1159588	0.07036197	0.013953930	0.0015307718
	$u_2(\eta)$	0.11595878	0.070361970	0.013953930	0.0015307713
	$u_2(\xi)$	0.11584326	0.069729793	0.013252970	0.0013097894
	$u_3(\xi)$	0.11584326	0.069729790	0.013252969	0.0013097907

Table 7(b). Shear stress at the lower and upper interfaces

Da		Da=1	Da=0.1	Da=0.01	Da=0.001
$\eta = 1/3$ $\xi = 2/3$	$\frac{du_1}{dy}(\eta)$	0.1513468697	0.07494555	-0.003034054	-0.00217397
	$\frac{du_2}{dy}(\eta)$	0.1513468658	0.0749456	-0.0030338	-0.0021
	$\frac{du_2}{dy}(\xi)$	-0.154591939	-0.0923160	-0.01383	0
	$\frac{du_3}{dy}(\xi)$	-0.154591941	-0.092315967	-0.013819155	$-8.3033708\,10^{-7}$
$\eta = 1/4$ $\xi = 3/4$	$\frac{du_1}{dy}(\eta)$	0.2304745740	0.13081715	0.011885128	-0.00135703
	$\frac{du_2}{dy}(\eta)$	0.230474552	0.130817149	0.011885174	-0.001384668
	$\frac{du_2}{dy}(\xi)$	-0.230391214	-0.130681377	-0.014963072	-4099.43426
	$\frac{du_3}{dy}(\xi)$	-0.230391213	-0.130681378	-0.014963467	66.4174053
$\eta = 0.49$ $\xi = 0.51$	$\frac{du_1}{dy}(\eta)$	0.0034674657	-0.026184815	-0.03398034	-0.01049068
	$\frac{du_2}{dy}(\eta)$	0.00346747194	-0.026184815	-0.03398034	-0.010490688
	$\frac{du_2}{dy}(\xi)$	-0.0148268056	-0.035881143	-0.03402269	-0.009796469
	$\frac{du_3}{dy}(\xi)$	-0.0148268147	-0.035881143	-0.03402269	-0.097964695

4.6. Mean velocity across the layers

The mean velocity across the layers is defined as:

$$\bar{u} = \bar{u}_1 + \bar{u}_2 + \bar{u}_3 = \int_0^{\eta} u_1 dy + \int_{\eta}^{\xi} u_2 dy + \int_{\xi}^{1} u_3 dy \tag{66}$$

where $\bar{u}_1, \bar{u}_2, \bar{u}_3$ are the mean velocities in layers 1, 2, and 3, respectively. Mean velocity calculations are illustrated for *Da* = 1 and different layer thicknesses in **Table 8.** This **Table** clearly shows the highest mean velocity being across the variable permeability layer for large thickness. This is due to the high flow rate in the middle layer, where a high permeability is associated with this layer. When the middle layer is thin, **Table 8** shows a decrease in the mean velocity across this layer due to the fact that permeability does not remain high enough to influence the mean velocity.

Table 8. Mean velocity across each porous layer and across the channel.

$\eta = 1/3$ $\xi = 2/3$	$\bar{u}_1$	0.020295189	$\eta = 1/4$ $\xi = 3/4$	$\bar{u}_1$	0.012253769	$\eta = 0.49$ $\xi = 0.51$	$\bar{u}_1$	0.037816843
	$\bar{u}_2$	0.080326876		$\bar{u}_2$	0.139845711		$\bar{u}_2$	0.0023977597
	$\bar{u}_3$	0.020028615		$\bar{u}_3$	0.012098218		$\bar{u}_3$	0.037401303
	$\bar{u}$	0.120650682		$\bar{u}$	0.164197699		$\bar{u}$	0.077615907

4.7. Velocity profiles across the layers

Velocity across the three layers is illustrated in **Fig. 4(a-c)** for different values of *n*, *Da* and *a* and *b*. For *Da* = 1, the velocity profile possesses a parabolic shape (**Fig. 4(a)**) that is lost with decreasing *Da*. As the product *bDa* decreases, or equivalently permeability in the upper layer decreases, and the product *aDa* increases, or equivalently permeability in the lower layer increases, velocity across the upper layer decreases and velocity across the lower layer increases, causing a loss in the parabolic velocity profile. This is true when *Da* decreases and assumes values below unity (**Figs. 4(b,c)**).

When *Da* = 1, the parabolic velocity profile is due to the dimensional permeability approaching infinity, and the flow is less affected by the introduction of a porous layer. The effect of increasing *n* is also illustrated in **Fig. 4(a-c)**, which demonstrate the increase in velocity in the middle layer with increasing *n*. Numerically, this is attributed to increasing permeability due to increasing *n* (as can be seen from equation (2), where the denominator is less the numerator, and the ratio in the permeability expression is greater than unity and increases by taking higher powers). Velocity in the middle layer and its dependence on *n* are further illustrated in **Figs. 5(a-c)**, which show the increase in velocity due to increasing permeability with increasing *n*, for given *Da*, *a* and *b*. Loss of parabolic shape with decreasing *Da* is also explained in terms of decreasing permeability in the upper bounding layer, which results in a slower flow in the upper part of the middle layer.

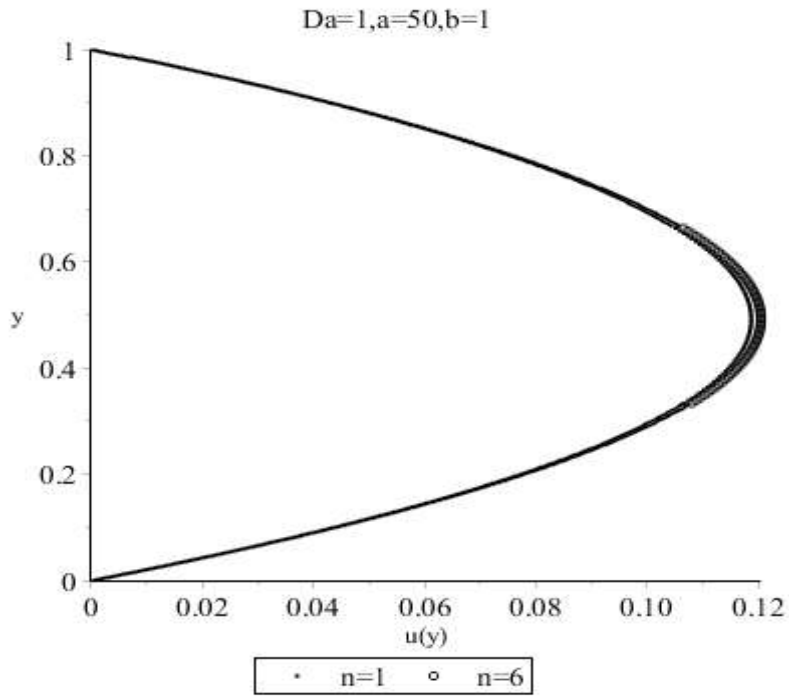

Figure 4(a) Velocity Profile u(y) ,for Da=1, $\eta = \frac{1}{3}, \xi = \frac{2}{3}$, a=50,b=1, different values of n.

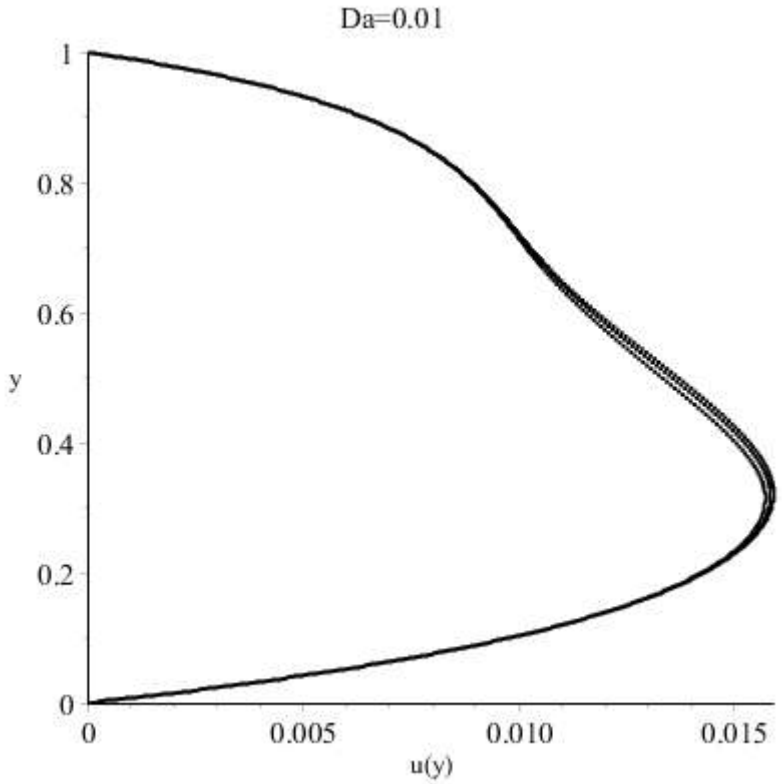

Figure 4(b) Velocity Profile u(y) ,for Da=0.01, $\eta = \frac{1}{3}, \xi = \frac{2}{3}$, a=2,b=1, different values of n.

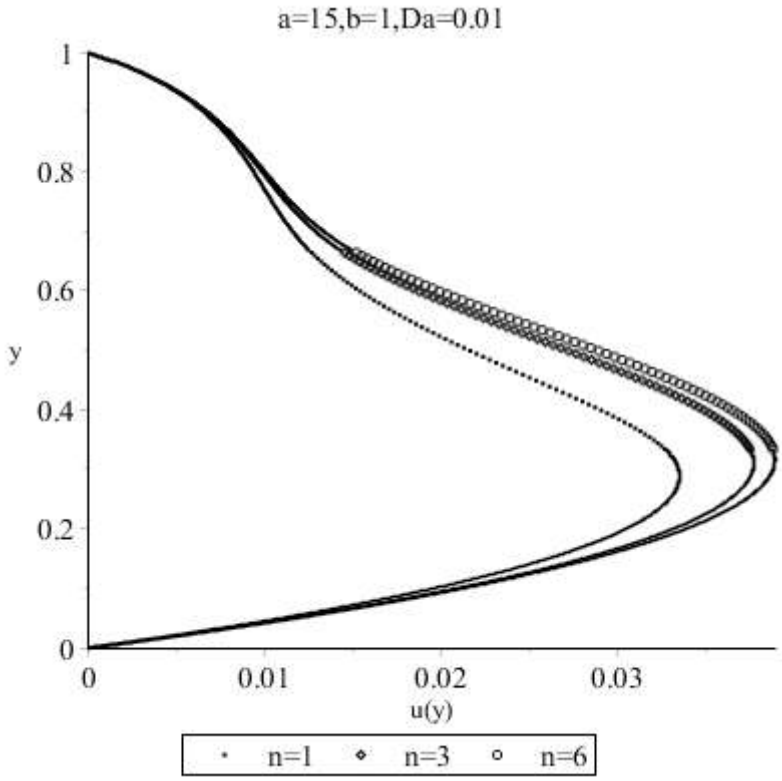

Figure 4(c) Velocity Profile u(y), for Da=0.01, $\eta = \frac{1}{3}, \xi = \frac{2}{3}$, a=2,b=1, different values of n.

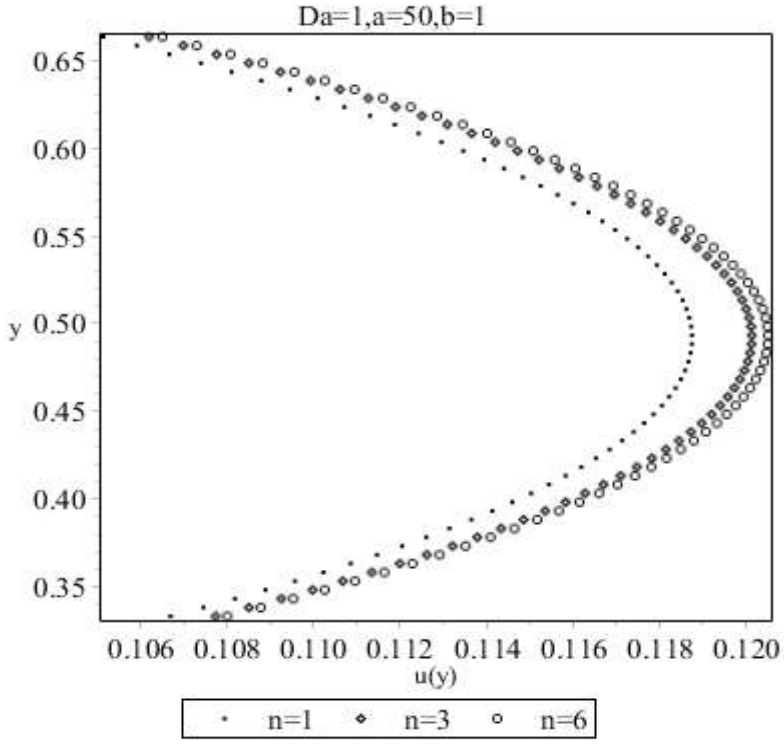

Figure 5(a) $u_2(y)$, **Da=1,** $\eta = \frac{1}{3}, \xi = \frac{2}{3}$, **a=50,b=1, and different values of n.**

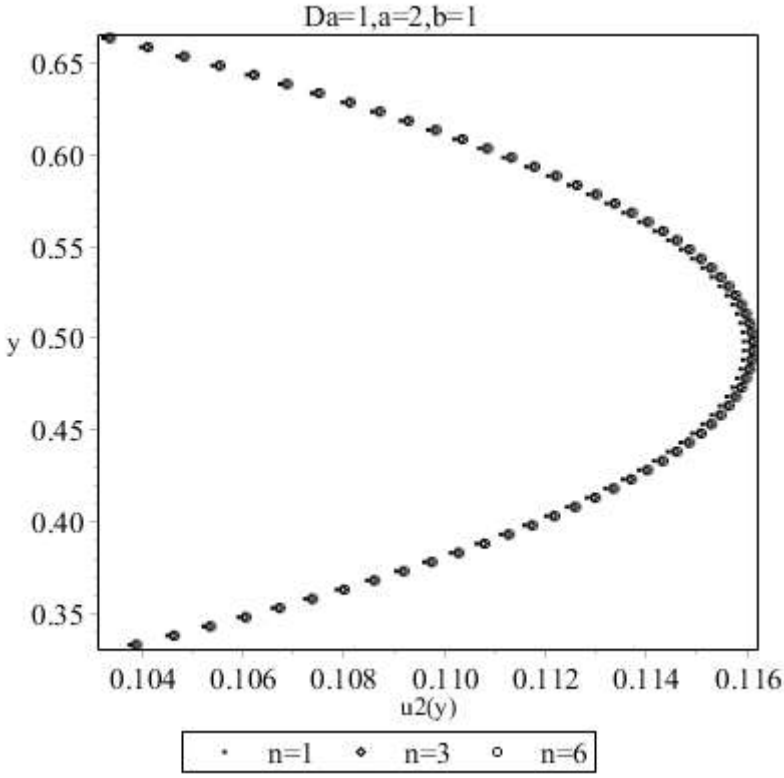

Figure 5(b) $u_2(y)$, **Da=1,** $\eta = \frac{1}{3}, \xi = \frac{2}{3}$, **a=2,b=1, and different values of n.**

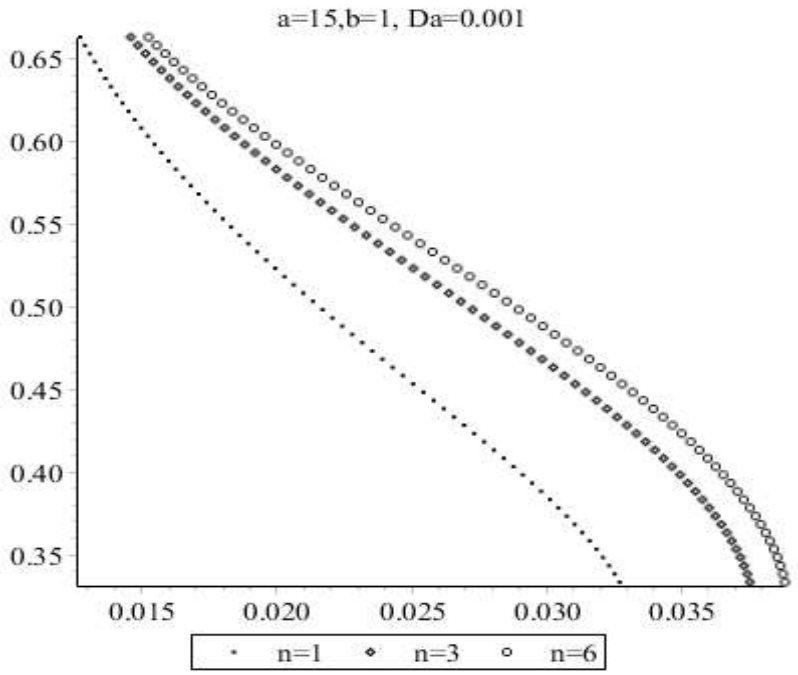

Figure 5(c): $u_2(y)$**, for Da=0.001,** $\eta = \frac{1}{3}, \xi = \frac{2}{3}$**, a=15,b=1, different values of n.**

5. CONCLUSION

In this work we considered the flow in a layered porous configuration, consisting of three layers the middle of which is of variable permeability. The bounding upper and lower layers are of constant permeability. This is the same configuration as that of the problem in [1] but with a permeability distribution in the middle layer that results in a generalized Airy's equation as the governing differential equation in the middle layer. This problem is undertaken to illustrate the effects of changing the power on the permeability expression (that is, the value of *n*) on the flow characteristics. The main conclusion reached here is that with increasing *n*, permeability in the middle layer increases and results in a corresponding increase in velocity.

REFERENCES

[1]. M. S. Abu Zaytoon, T. L. Alderson, M. H. Hamdan, Flow through layered media with embedded transition porous layer, Int. J. of Enhanced Research in Science, Technology & Engineering vol. 5 Issue 4, pp. 9-26, April-2016.

[2]. M. S. Abu Zaytoon, T. L. Alderson and M. H. Hamdan, Flow over a Darcy porous layer of variable Permeability, Journal of Applied Mathematics and Physics, vol. 4, pp. 86-99, 2016.

[3]. M. S. Abu Zaytoon, T. L. Alderson and M. H. Hamdan, Flow through a variable permeability Brinkman porous core, Journal of Applied Mathematics and Physics, vol. 4, pp. 766-778, 2016.

[4]. M.S. Abu Zaytoon, Flow through and over Porous Layers of Variable Thicknesses and Variable Permeability, PhD Thesis, University of New Brunswick, Saint John, Canada, 2015.

[5]. A.H.-D. Cheng, Darcy's flow with variable permeability: a boundary integral solution, Water Resources Res., vol. 20(7), pp. 980-984, 1984.

[6]. M.H. Hamdan, and M.T. Kamel, Flow through variable permeability porous layers, Adv. Theor. Appl. Mech., vol. 4(3), pp. 135-145, 2011.

[7]. D. A. Nield and A. V. Kuznetsov, The effect of a transition layer between a fuid and a porous medium: shear flow in a channel, Transport in Porous Media, vol. 78, pp. 477-487, 2009.

[8]. M. Abramowitz and I.A. Stegun, Handbook of Mathematical Functions, Dover, New York, 1984.

[9]. M.H. Hamdan and M.T. Kamel, On the Ni(x) integral function and its application to the Airys non-homogeneous equation, Appl. Math. Comput., vol. 217, pp. 7349-7360, 2011.

[10]. C.A. Swanson and V. B. Headley, An extension of Airy's equation. SIAM J. Appl. Math. Vol. 15, pp. 1400-1412, 1967.